CrossMark

ORIGINAL PAPER

α-D-Glucopyranose Adsorption on a Pd$_{30}$ Cluster Supported on Boron Nitride Nanotube

Antonio Prestianni[1] · Remedios Cortese[1] · Francesco Ferrante[1] · Roberto Schimmenti[1] ·
Dario Duca[1] · Sophie Hermans[2] · Dmitry Yu. Murzin[3]

Abstract Boron nitride nanotube (BNNT) as an innovative support for carbohydrate transformation processes was evaluated, using density functional theory. The α-D-glucopyranose adsorption on a Pd$_{30}$ cluster, supported on BNNT, was used to check both the local activity of topologically different metallic sites and the effects of the proximity of the BNNT surface to the same metallic sites. Detailed geometrical and electronic analyses performed on Pd$_{30}$/BNNT and α-D-glucopyranose/Pd$_{30}$/BNNT systems were discussed. It was observed that the deposition of the Pd$_{30}$ cluster onto the BNNT support gives rise to an electronic rearrangement, determining a charge transfer from the support to the adsorbed metal cluster. The charge transfer, as shown by the analysis of molecular electrostatic potential, seems to generate electron-rich and electron-poor zones in the Pd$_{30}$ cluster. The α-D-glucopyranose species, regardless the interaction geometry experienced, acts as an electron donor and preferentially adsorbs close to the electron-poor metal/support interface.

Keywords Boron nitride nanotube · Supported palladium catalyst · α-D-Glucopyranose adsorption · Surface site reactivity · DFT · Molecular electrostatic potential

✉ Dario Duca
dario.duca@unipa.it

1 Dipartimento di Fisica e Chimica, Università degli Studi di Palermo, Viale delle Scienze Ed. 17, 90128 Palermo, Italy

2 Institut de la Matière Condensée et des Nanosciences (IMCN), Université Catholique de Louvain, Place Louis Pasteur 1, 1348 Louvain-la-Neuve, Belgium

3 Laboratory of Industrial Chemistry and Reaction Engineering, Process Chemistry Centre, Åbo Akademi University, Biskopsgatan 8, 20500 Turku, Finland

1 Introduction

The complete understanding of the principles that rule the behavior of a supported catalyst cannot be reached without a deep analysis of the effect exerted by the support itself. An impressive example is represented by the strong metal-support interaction (SMSI) effects. SMSI, firstly introduced by Tauster [33], thanks to the improvement of usable experimental techniques and to the synergy of experiments and computational simulations, has been widely investigated and discussed during the last 25 years [4, 25, 36, 38]. It seems, out of any doubt, that the electronic effects play a crucial role in determining the activity of supported metal particles [5, 26, 28, 30, 37], also when the latter are not so strongly adsorbed on the support. The wide majority of the metal/support interaction studies deals usually with metal oxides, such as titania and alumina, but recently new layered and tubular materials have started to draw more interest.

Among these, due to their advantageous mechanical and thermal properties, boron nitride based nanotubes (BNNT) seem to be promising for their use as catalytic supports [2, 15, 18, 34]. In particular, the lack of acidic sites could avoid the local sintering of the supported metals, as it is often encountered if metal oxides are used [27]. The potential use of boron nitrides as catalyst support has been previously evaluated by Meyer et al. [22–24] using palladium as active phase in the case of both oxidation and hydrogenation of lactose. It has been shown that the support may affect the reaction activity and selectivity, resulting in better performance of the catalyst.

Computational methods used to model a large palladium cluster, showing planes with different indexing that interact with a boron nitride surface could unveil the influence of the metal and the support on the catalytic properties of the

resulting materials. One of the most interesting implication of this approach is the possibility to study how molecules of high industrial interest interact with the different metallic planes of the supported metal cluster. To the best of our knowledge the few computational studies already performed in literature, on these kind of systems, mainly concern the adsorption of small molecules, such as hydrogen, onto BNNT supported metallic clusters [41], while oxygenates such as α-D-glucopyranose, despite their high catalytic interest in the biomass conversion technology, were rarely treated [3, 8]. Moreover, α-D-glucopyranose is also a representative molecule suitable to capture the main chemical features of oxygenates in the biomass. As already reported [22, 23], it was actually suggested that the adsorption process of saccharides on palladium clusters could be shape sensitive, preferentially occurring on the surface of the cluster, while edge and corners on the metal nanoparticle could exert a detrimental effect on the above mentioned reactions [24].

In order to deepen the topics above, a computational study addressed to simulate the adsorption of α-D-glucopyranose molecule on a model heterogeneous catalyst formed by a Pd_{30} cluster supported on a BNNT surface, is presented. By the use of a properly shaped Pd cluster it was possible to evaluate the influence of different low Miller-index planes upon adsorption. Furthermore, in order to predict the effect of the electronic metal/support interactions on the adsorption of the α-D-glucopyranose, we analyzed the characteristics of the molecular electrostatic potential (MEP) of the involved systems, which is related to the local charge distribution and allows one a straightforward identification of relevant active sites of the supported cluster [1].

2 Computational Details

A Pd_{30} cluster was chosen to model the metal catalyst whereas a (12,12) armchair single walled nanotube was chosen to mimic the BNNT support. The metallic fragment, cut out from the fcc bulk Pd structure, was purposely shaped so as to expose both the (111) and (100) planes [10, 29]. The curvature and the total length in the axial direction of the model support were selected because it allowed us to treat efficiently the system formed by α-D-glucopyranose adsorbed on the Pd_{30}/BNNT aggregate. According to our recent studies, the effects of the curvature on the adsorption process of small clusters on BNNT seems to be negligible [32]. It is therefore very likely that the influence of the modeled nanotube curvature could be even less evident on molecules adsorbed on metal clusters supported on it.

With regard to the D-glucose molecule, it is important to remind that it can exist in five tautomeric forms (two pyranosic, two furanosic and one aldehydic) and each of them present a very high conformational flexibility, already widely investigated in the literature. While early results showed that more than 700 conformations are possible [9], the D-glucose in water is found almost exclusively in the α closed pyranose form. Even considering that the conformational ensemble of the α-D-glucopyranose could be small if adsorbed on a metal surface as, for example, already found for similar sugars adsorbed on ruthenium [7], the number of different conformations to take into account in a systematic investigation would be prohibitively high. For this reason, in the present study we used only the most stable α-D-glucopyranose conformation obtained in gas phase by Corchado et al. [6] through a combined molecular dynamics and DFT study. In the following, the conventional α-D-glucopyranose carbon atoms numeration is used.

All the calculations were performed by using the Gaussian 09 code [14]. Due to the size of the investigated system the 2-layer ONIOM QM/MM approach [11] was found to be well suited. The corresponding model system was a circumcoronene-like $B_{27}N_{27}$ portion of a (12,12) armchair single walled BNNT formed on the whole by 12 unit cells. Since the performed calculations were not periodic, the dangling bonds on the terminal sides of the nanotube were saturated by hydrogen atoms. Molecular mechanics employing the Universal Force Field (UFF) [31] was used as the low level method in the ONIOM prescription, while DFT was selected for the high level. The exchange–correlation functional chosen is the hybrid Coulomb-attenuated CAM-B3LYP [39]; this was joined with the Los Alamos LANL2 effective core potential for the Pd atoms, with the corresponding double-ζ valence basis set, and the dunning D95V basis set for B, N, C, O and H. Full geometry relaxation was carried out on the systems resulting from the adsorption on the BNNT of the Pd_{30} cluster and of α-D-glucopyranose on Pd_{30}/BNNT. The adsorption energy of a Pd_{30} cluster on the BNNT was obtained through the general formula:

$$\Delta E^{Ads} = E_{Pd/BN} - E_{BN} - E_{Pd} \tag{1}$$

where $E_{Pd/BN}$ is the total energy of the supported cluster system, E_{BN} the energy of the pristine BNNT support fragment and E_{Pd} the energy of the isolated Pd_{30} cluster. The adsorption energy of the α-D-glucopyranose on the supported Pd_{30} cluster was conversely obtained through the general formula:

$$\Delta E_{G/Pd/BN}^{Ads} = E_{G/Pd/BN} - E_{Pd/BN} - E_G \tag{2}$$

being $E_{G/Pd/BN}$ the energy of the pyranosyde adsorbed on the Pd_{30}/BNNT system, $E_{Pd/BN}$ the energy of the Pd_{30}/

BNNT system and E_G the energy of the isolated α-D-glucopyranose.

3 Results and Discussion

3.1 Adsorption of Pd$_{30}$ Cluster

The interaction geometry of the Pd$_{30}$ cluster on the BNNT was designed in order to allow the exposure of the (111) and (100) planes to adsorption; the remaining surface, i.e. a (111) plane, was placed in contact with the support (see Fig. 1a).

The adsorption geometry of the supported Pd$_{30}$ cluster can be analyzed considering the matching-points of the interacting (111) Pd plane with the BNNT. For other supported metallic systems, it was already shown that complementary symmetries, characterizing cluster faces and support surfaces, are significant driving forces, which leads to effective interactions between them [40]. This criterion has been also employed to understand the growth mechanism of h-BN nanosheets on low Miller-index planes of different metals, driving at the conclusion that negligible lattice mismatches give raise to stronger adsorption [19].
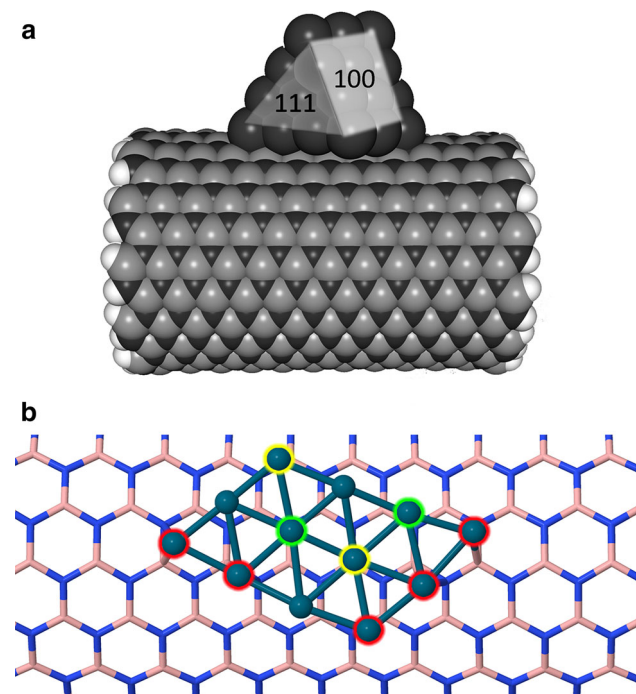

Fig. 1 Pd$_{30}$/BNNT model system: **a** optimized structure, **b** details of the interaction points between the first layer of the palladium cluster and the BNNT support: the *red* shaded Pd atoms have a bridge coordination while the *yellow* and the *green* shaded ones are atop coordinated to boron and nitrogen, respectively

According to the investigation reported by Schimmenti et al. [32], the Pd–N interactions are preferred to the Pd–B ones. Thus, the favored surface configuration should be the one where the metal particle maximizes the number of atop coordinations of the Pd atoms with the nitrogens. This is also found for the opposite case in which the growth of a boron nitride sheet on a close packed metal surface is considered, indeed yielding $N_{atop}B_{fcc/hcp}$ configurations. Analyzing the geometrical features of the Pd$_{30}$/BNNT structure, it can be noted that the palladium (111) plane in contact with the BNNT support is characterized by a sensible lattice mismatch with the surface of the latter. Nevertheless, an adsorption energy of −120 kJ mol^{-1} was found. To make a qualitative comparison with other supports, Kacprzak et al. [17] for the adsorption of a Pd$_9$ cluster on γ-Al$_2$O$_3$ found a value of ca. −300 kJ mol^{-1} while Duca et al. [13] for the same palladium cluster adsorbed on a carbon nanotube pinpointed a BSSE corrected interaction energy of about −230 kJ mol^{-1}. The large difference of the observed adsorption energy values is in agreement with previous studies in which a weaker interaction of metals with boron nitride support, compared to γ-Al$_2$O$_3$, was suggested [20]. The difference above could be attributed to the absence of oxygenated moieties in the BN supports. This straightforwardly reduces the interaction ability of the BN surface, but at the same time also decreases its chances to promote side-reactions in catalytic oxidations thus enhancing the overall selectivity of the corresponding metal supported catalysts [23].

Due to the different Pd–Pd and B–N bond lengths, some distortions of the cluster structure have to occur in order to have a best possible cluster-support matching. For this reason, the Pd atoms interacting with the surface are mainly corner atoms which are connected by a two fold coordination with BNNT boron and nitrogen atoms characterized, irrespective of the surface atom involved, by a bond distance of ca. 2.8 Å. Longer range Pd–N interactions, with average bond distance of 3.1 Å, are also present (see Fig. 1b). The global effect of the adsorption on the BNNT surface can be conclusively associated to a screw displacement of the Pd cluster (100) plane toward the exposed (111).

As a final remark, it can be observed that, according to a population analysis based on natural orbitals (NBO), a charge transfer of −0.14e occurs from the BNNT to the metal cluster. This electronic charge donation may be related to the experimentally observed beneficial effect that the BNNT support exerts on palladium deactivation. Indeed, it was shown that boron nitride lattice stabilizes palladium clusters in their reduced form [22, 23], in this way enhancing the lactose selective oxidation. The detrimental effects of oxidation on the palladium catalytic properties was confirmed by Murzin et al. [35] and more

recently by Delidovich et al. [12] that studied selective oxidation, respectively, of lactose and glucose over Pd/C, observing catalyst deactivation attributable to the formation of surface Pd(II) oxide. In addition, when preparing Pd/C catalysts by grafting of Pd(II) complexes by surface ligand exchange on functionalized carbon supports, Hermans et al. have noticed that the Pd(II) form becomes stabilized and oxygenated surface groups remain on the support [16, 21].

3.2 Adsorption of α-D-Glucopyranose onto the Cluster

Analyzing the three-dimensional structure of the considered conformation of the D-glucose α pyranosic ring it is possible to single out two non-equivalent profiles, whose differences are mainly produced by the OH group positions, imposed by the chirality of the carbon atoms. When this molecule approaches the metallic surface during the adsorption process, at least two limit geometries for the binding modes can be identified. One of this, is characterized by the CH_2OH group pointing toward the surface (G^1) whereas the other shows the hydroxy-methyl group far from the surface (G^2). In order to investigate the shape selectivity of the adsorption process, the two binding modes were studied on the two different surfaces exposed by the palladium cluster. The four resulting configurations, $G^1_{(111)}$, $G^2_{(111)}$, $G^1_{(100)}$, and $G^2_{(100)}$ were fully relaxed, giving the optimized structures reported in Fig. 2.

The calculated adsorption energies for the four systems are reported in Table 1. It is possible to note that the G^2 binding mode is almost equivalent for both the considered metallic planes whereas in the G^1 case, the interaction with the (111) plane seems to be preferential. The G^1, corresponding to the most stable configuration, is distinguished for multipoint interactions of the α-D-glucopyranose with the cluster via three hydroxylic moieties (Pd–O_6 2.21, Pd–O_4 2.42, Pd–O_1 2.37 Å); whereas almost isoenergetic $G^2_{(111)}$, $G^1_{(100)}$, and $G^1_{(111)}$ show only a single interaction via one hydroxyl group (Pd–O, 2.28 Å, Pd–O_6, 2.25 Å and Pd–O_3 2.19 Å, respectively). This trend can be explained taking into account (i) the number of OH groups on the two sides of the α-D-glucopyranose molecule and (ii) the matching between the OH arrangement and the topology of the exposed surface. The first affects the interaction geometry of the two surface binding modes, the second conversely rules the occurrence of single or multiple adsorption on the two metallic planes. It is interesting to note that along the adsorption process, the conformation of α-D-glucopyranose is retained, irrespective of the implicated binding modes [7]. Very similar geometries and interaction energies are found if the α-D-glucopyranose

adsorbs on the unsupported Pd_{30}. In particular, the adsorption energy for the G^1 configuration is essentially unchanged while for the other binding modes a small increase (ca. 10 kJ mol^{-1}) can be noticed when the support is included in the system.

Due to the high ratio between the low and high coordinated sites in the Pd_{30} cluster, the OH groups of the adsorbed molecule interact mainly with Pd edge sites. For sake of completeness it has to be highlighted that in the literature it was suggested that adsorption on low coordinated sites produces deleterious effects towards oxidation of lactose: as observed experimentally, smaller palladium particles (<3 nm) are actually less active than larger ones (5 nm) [22, 23]. This issue is outside of the main focus of the present study since the model was explicitly conceived to investigate the support effects on the adsorption process of the α-D-glucopyranose and not to unravel the reaction mechanism of its oxidation.

In order to rationalize the combined effects on the metal cluster produced by both the support and the adsorbate, it is helpful to analyze the trend of the charge transfers, evaluated by means of a NBO analysis. As reported in the previous section the BNNT donates to the cluster −0.14e. According to the calculations performed on the unsupported Pd_{30}, the charge transferred from the adsorbate to the cluster is −0.29, −0.26 and −0.31e, for the $G^1_{(100)}$, $G^2_{(100)}$ and $G^2_{(111)}$ modes, and −0.47e in the $G^1_{(111)}$.

These charge transfers to the Pd_{30} cluster are almost additive when the α-D-glucopyranose/Pd_{30}/BNNT system is considered, being their magnitudes −0.43, −0.41, −0.50 and −0.66e for the $G^1_{(100)}$, $G^2_{(100)}$, $G^2_{(111)}$ and $G^1_{(111)}$ configurations, respectively. The latter binding mode shows the largest negative charge transfer in virtue of its three-point interaction.

The investigated systems show a high degree of complexity since there are multiple and interrelated effects, arising by the support, the adsorbate and the metallic cluster. In order to describe local electron density depletion or rise on the cluster, which could correspond to different reactivity areas on the catalyst surface, the analysis of the molecular electrostatic potential maps is more informative than the simple net charge transfer.

As reported in Fig. 3 the deposition of the palladium cluster on the BNNT generates a rearrangement of the Pd_{30} MEP, which actually shows more and more negative values, going from the first metallic layer (i.e. the layer in contact with the support) to the last one. Even if, on the whole, there is a charge transfer from the BNNT to the cluster that could, in principle, inhibit the interaction with the α-D-glucopyranose, the presence of localized electron depletion zones guarantees an effective interaction between metal cluster and adsorbate. This implies that regions of the

Fig. 2 Optimized structures of the α-D-glucopyranose adsorbed on the two exposed metallic faces of the Pd_{30}/BNNT model: **a** $G^2_{(100)}$, **b** $G^2_{(111)}$, **c** $G^1_{(100)}$, **d** $G^1_{(111)}$
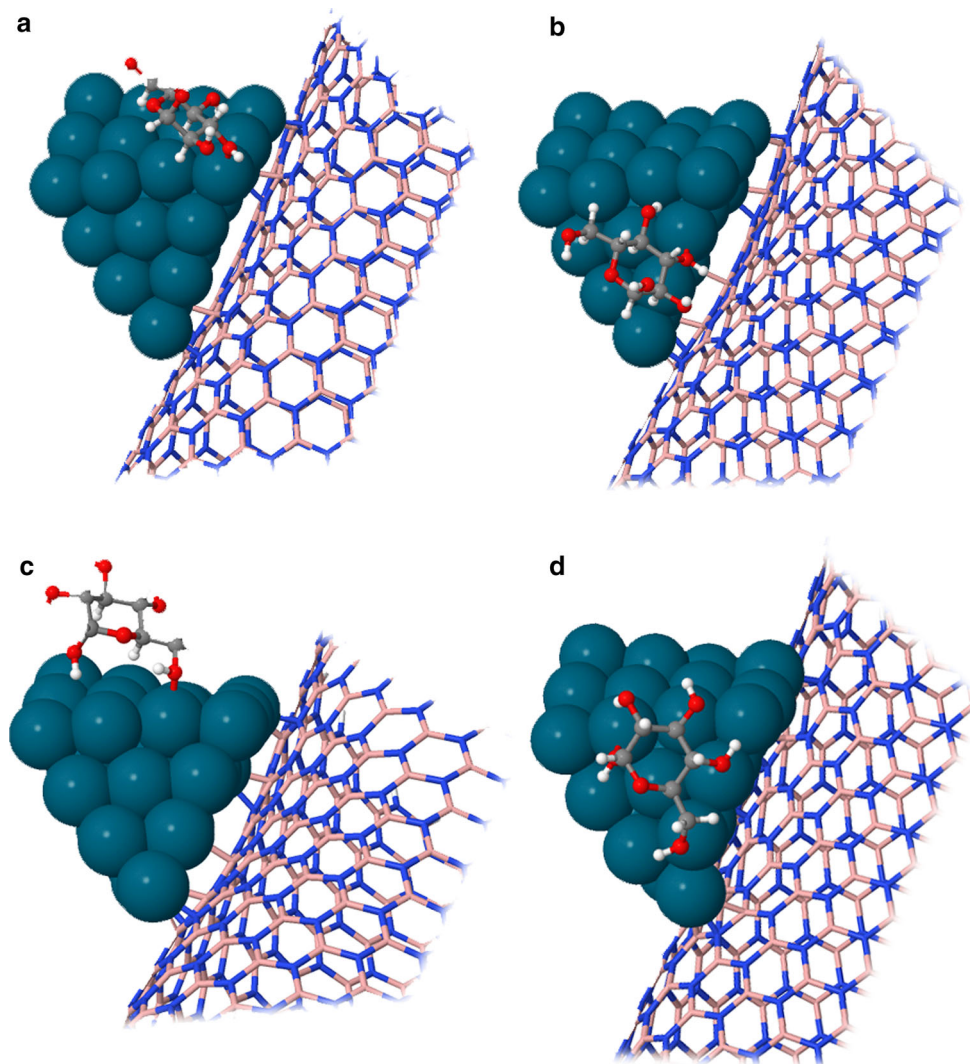

Table 1 Adsorption energies (kJ mol^{-1}) of the four α-D-glucopyranose binding modes on supported and unsupported Pd_{30} cluster

	$G^1_{(100)}$	$G^2_{(100)}$	$G^2_{(111)}$	$G^1_{(111)}$
Pd_{30}	−91.8	−97.2	−98.9	−150.0
Pd_{30}/BNNT	−107.9	−109.1	−111.2	−152.5

cluster closer to the support surface could be more prone to interact with the hydroxyl moieties belonging to the α-D-glucopyranose, as also suggested by the optimized geometries reported in Fig. 2. It is possible therefore that some contribution to the total adsorption energy comes from the interaction of the glucopyranose with the support. In order to evaluate the size of this contribution the system formed by the α-D-glucopyranose directly adsorbed on the BNNT has been optimized, and the interaction energy
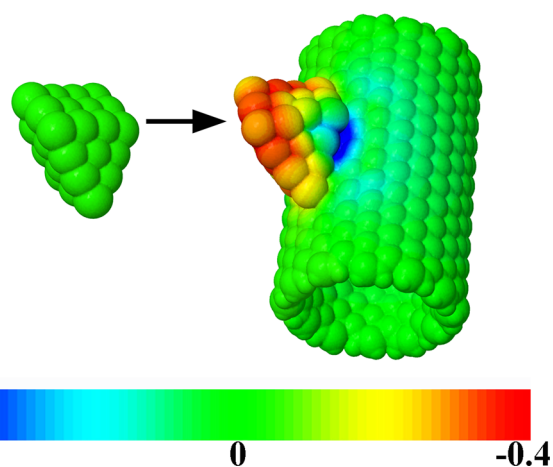

Fig. 3 Molecular electrostatic potential (*Eh/e*) of the isolated Pd_{30} cluster and of the Pd_{30}/BNNT system
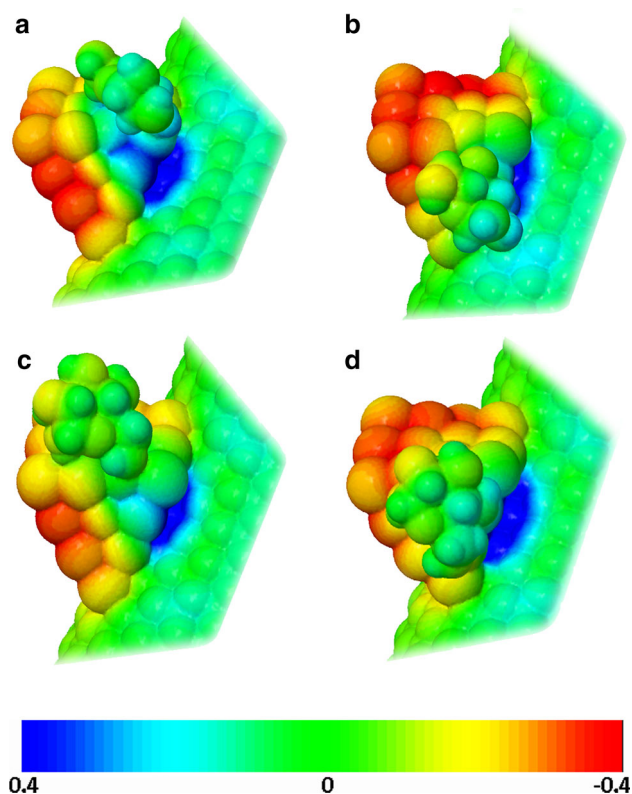
Fig. 4 Molecular electrostatic potential (*Eh/e*) of the α-D-glucopyranose/Pd$_{30}$/BNNT systems: **a** G$^2_{(100)}$, **b** G$^2_{(111)}$, **c** G$^1_{(100)}$, **d** G$^1_{(111)}$

population analysis, the support would seem to transfer electron density to the adsorbed metal cluster. This charge shift could be related to the experimentally claimed ability of the BN supports to stabilize the reduced form of the Pd component, characterizing the corresponding supported catalysts. The analysis of four different binding modes of α-D-glucopyranose on the palladium cluster showed that the conformation of the α anomer is retained along with the adsorption process, which also is characterized by a quite high interaction energy. According to our analysis, the α-D-glucopyranose, irrespective of its interaction geometry, acts as an electron donor. Molecular electrostatic potential maps show that when adsorbed on BNNT, the Pd$_{30}$ cluster exhibits a peculiar electron-rich surface area together with an electron-poor area. This latter is localized at the metal-support interface, which is where the α-D-glucopyranose preferentially adsorbs. The investigation on the role of the support and the characterization of the adsorption geometry and energetics, besides giving insights on the adsorption process itself, should be intended also as a source of information of valuable interest if framed within a context devoted to analyze reaction mechanisms of D-glucose on supported palladium catalysts.

resulted only -30 kJ mol^{-1}. Thus, it can be supposed that the contribution above is much smaller than this value, pointing a minor direct influence of the support to the overall adsorption energy.

The adsorption of α-D-glucopyranose clearly modifies the appearance of the MEP, as reported in Fig. 4. The palladium atoms interacting with the molecular adsorbate show a more positive electrostatic potential if compared to the edge sites far from the interface. This suggests that possibly electron withdrawing species could interact more easily with edge sites far from the interface cluster support. Interestingly, this molecular electrostatic potential anisotropy might be connected with the hypothesis, which relates the higher activity of palladium catalyst toward lactose hydrogenation to the preferential adsorption of hydrogen on low coordinated sites [24].

4 Conclusions

Aiming at understanding the role of the support in the Pd/BNNT catalysts, DFT calculations on Pd$_{30}$/BNNT and α-D-glucopyranose/Pd$_{30}$/BNNT molecular systems were performed. The results pointed out several indications on the nature of metal-support interactions. According to NBO

References

1. Armaković SJ, Armaković S, Finčur NL, Šibul F, Vione D, Šetrajčić JP, Abramović BF (2015) Influence of electron acceptors on the kinetics of metoprolol photocatalytic degradation in TiO$_2$ suspension: a combined experimental and theoretical study. RSC Adv 5:54589–54604
2. Becton M, Wang X (2015) Grain-size dependence of mechanical properties in polycrystalline boron–nitride: a computational study. Phys Chem Chem Phys 17:21894–21901
3. Besson M, Gallezot P, Pinel C (2014) Conversion of biomass into chemicals over metal catalysts. Chem Rev 114:1827–1870
4. Bruix A, Rodriguez JA, Ramìrez PJ, Senanayake SD, Evans J, Park JB, Stacchiola D, Liu P, Hrbek J, Illas F (2012) A new type of strong metal-support interaction and the production of H$_2$ through the transformation of water on Pt/CeO$_2$(111) and Pt/CeO$_x$/TiO$_2$(110) catalysts. J Am Chem Soc 134:8968–8974
5. Campbell CT (2012) Catalyst-support interactions: electronic perturbations. Nat Chem 4:597–598
6. Corchado JC, Sànchez ML, Aguilar MA (2004) Theoretical study of the relative stability of rotational conformers of α and β-D-glucopyranose in gas phase and aqueous solution. J Am Chem Soc 126:7311–7319
7. Cortese R, Duca D, Sifontes Herrera VA, Murzin DY (2012) L-arabinose conformers adsorption on ruthenium surfaces: a DFT study. J Phys Chem C 116:14908–14916
8. Cortese R, Schimmenti R, Armata N, Ferrante F, Prestianni A, Duca D, Murzin DY (2015) Investigation of polyol adsorption on Ru, Pd, and Re using vdW density functionals. J Phys Chem C 119:17182–17192
9. Cramer CJ, Truhlar DG (1993) Quantum chemical conformational analysis of glucose in aqueous solution. J Am Chem Soc 115:5745–5753

10. Crespo-Quesada M, Yoon S, Jin M, Prestianni A, Cortese R, Càrdenas-Lizana F, Duca D, Weidenkaff A, Kiwi-Minsker L (2015) Shape-dependence of Pd nanocrystal carburization during acetylene hydrogenation. J Phys Chem C 119:1101–1107

11. Dapprich S, Komàromi I, Byun KS, Morokuma K, Frisch MJ (1999) A new ONIOM implementation in Gaussian98. Part I. The calculation of energies, gradients, vibrational frequencies and electric field derivatives. J Mol Struct THEOCHEM 461–462:1–21

12. Delidovich IV, Taran OP, Matvienko LG, Simonov AN, Simakova IL, Bobrovskaya AN, Parmon VN (2010) Selective oxidation of glucose over carbon-supported Pd and Pt catalysts. Catal Lett 140:14–21

13. Duca D, Ferrante F, La Manna G (2007) Theoretical study of palladium cluster structures on carbonaceous supports. J Phys Chem C 111:5402–5408

14. Frisch MJ, Trucks GW, Schlegel HB, Scuseria GE, Robb MA, Cheese-man JR, Scalmani G, Barone V, Mennucci B, Petersson GA, Nakatsuji H, Caricato M, Li X, Hratchian HP, Izmaylov AF, Bloino J, Zheng G, Sonnenberg JL, Hada M, Ehara M, Toyota K, Fukuda R, Hasegawa J, Ishida M, Nakajima T, Honda Y, Kitao O, Nakai H, Vreven T, Montgomery JA Jr, Peralta JE, Ogliaro F, Bearpark M, Heyd JJ, Brothers E, Kudin KN, Staroverov VN, Kobayashi R, Normand J, Raghavachari K, Rendell A, Burant JC, Iyengar SS, Tomasi J, Cossi M, Rega N, Millam JM, Klene M, Knox JE, Cross JB, Bakken V, Adamo C, Jaramillo J, Gomperts R, Stratmann RE, Yazyev O, Austin AJ, Cammi R, Pomelli C, Ochterski JW, Martin RL, Morokuma K, Zakrzewski VG, Voth GA, Salvador P, Dannenberg JJ, Dapprich S, Daniels AD, Farkas Ö, Foresman JB, Ortiz JV, Cioslowski J, Fox DJ (2009) Gaussian09 revision D.01. Gaussian Inc., Wallingford

15. Gao N, Fang X (2015) Synthesis and development of graphene–inorganic semiconductor nanocomposites. Chem Rev 115(16):8294–8343

16. Hermans S, Diverchy C, Dubois V, Devillers M (2014) Pd nanoparticles prepared by grafting of Pd complexes on phenol-functionalized carbon supports for liquid phase catalytic applications. Appl Catal A 474:263–271

17. Kacprzak KA, Czekaj I, Mantzaras J (2012) DFT studies of oxidation routes for Pd$_9$ clusters supported on γ-alumina. Phys Chem Chem Phys 14:10243–10247

18. Kim KS, Kingston CT, Hrdina A, Jakubinek MB, Guan J, Plunkett M, Simard B (2014) Hydrogen-catalyzed, pilot-scale production of small-diameter boron nitride nanotubes and their macroscopic assemblies. ACS Nano 8:6211–6220

19. Koitz R, Norskov JK, Studt F (2015) A systematic study of metal-supported boron nitride materials for the oxygen reduction reaction. Phys Chem Chem Phys 17:12722–12727

20. Lin CA, Wu JCS, Pan JW, Yeh CT (2002) Characterization of boron–nitride-supported Pt catalysts for the deep oxidation of benzene. J Catal 210:39–45

21. Mager N, Meyer N, Léonard AF, Job N, Devillers M, Hermans S (2014) Functionalization of carbon xerogels for the preparation of palladium supported catalysts applied in sugar transformations. Appl Catal B 148–149:424–435

22. Meyer N, Bekaert K, Pirson D, Devillers M, Hermans S (2012) Boron nitride as an alternative support of Pd catalysts for the selective oxidation of lactose. Catal Commun 29:170–174

23. Meyer N, Pirson D, Devillers M, Hermans S (2013) Particle size effects in selective oxidation of lactose with Pd/h-BN catalysts. Appl Catal A 467:463–473

24. Meyer N, Devillers M, Hermans S (2015) Boron nitride supported Pd catalysts for the hydrogenation of lactose. Catal Today B 241:200–207

25. Murzin DY (1995) On the kinetic interpretation of metal-support interaction. React Kinet Catal Lett 55:275–281

26. Pacchioni G (2013) Electronic interactions and charge transfers of metal atoms and clusters on oxide surfaces. Phys Chem Chem Phys 15:1737–1757

27. Postole G, Gervasini A, Guimon C, Auroux A, Bonnetot B (2006) Influence of the preparation method on the surface characteristics and activity of boron–nitride-supported noble metal catalysts. J Phys Chem B 110:12572–12580

28. Prestianni A, Ferrante F, Simakova OA, Duca D, Murzin DY (2013) Oxygen-assisted hydroxymatairesinol dehydrogenation: a selective secondary-alcohol oxidation over a gold catalyst. Chem Eur J 19:4577–4585

29. Prestianni A, Crespo-Quesada M, Cortese R, Ferrante F, Kiwi-Minsker L, Duca D (2014) Structure sensitivity of 2-methyl-3-butyn-2-ol hydrogenation on Pd: computational and experimental modeling. J Phys Chem C 118:3119–3128

30. Prestianni A, Ferrante F, Sulman EM, Duca D (2014) Density functional theory investigation on the nucleation and growth of small palladium clusters on a hyper-cross-linked polystyrene matrix. J Phys Chem C 118:21006–21013

31. Rappe AK, Casewit CJ, Colwell KS, Goddard WA, Skiff WM (1992) UFF, a full periodic table force field for molecular mechanics and molecular dynamics simulations. J Am Chem Soc 114:10024–10035

32. Schimmenti R, Cortese R, Ferrante F, Prestianni A, Duca D (2016) Growth of sub-nanometric palladium clusters on boron nitride nanotubes: a DFT study. Phys Chem Chem Phys 18:1750–1757

33. Tauster SJ (1987) Strong metal-support interactions. Acc Chem Res 20:389–394

34. Terrones M, Romo-Herrera JM, Cruz-Silva E, Lòpez-Urìas F, Munõz- Sandoval E, Velàzquez-Salazar JJ, Terrones H, Bando Y, Golberg D (2007) Pure and doped boron nitride nanotubes. Mater Today 10:30–38

35. Tokarev AV, Murzina EV, Kuusisto J, Mikkola J-P, Eranen K, Murzin DY (2006) Kinetic behaviour of electrochemical potential in three- phase heterogeneous catalytic oxidation reactions. J Mol Catal A 255:199–208

36. Venezia AM, Duca D, Floriano MA, Deganello G, Rossi A (1992) Chemical effect on the XPS spectra of the valence band and on O KLL and Pd MNN Auger spectra in pumice-supported catalysts. Surf Interface Anal 18:619–622

37. Wang YG, Yoon Y, Glezakou VA, Li J, Rousseau R (2013) The role of reducible oxide-metal cluster charge transfer in catalytic processes: new insights on the catalytic mechanism of CO oxidation on Au/TiO$_2$ from ab initio molecular dynamics. J Am Chem Soc 135:10673–10683

38. Willinger MG, Zhang W, Bondarchuk O, Shaikhutdinov S, Freund HJ, Schlögl R (2014) A case of strong metal-support interactions: combining advanced microscopy and model systems to elucidate the atomic structure of interfaces. Angew Chem Int Ed 53:5998–6001

39. Yanai T, Tew DP, Handy NC (2004) A new hybrid exchange–correlation functional using the coulomb-attenuating method (CAM–B3LYP). Chem Phys Lett 393:51–57

40. Zhang J, Alexandrova AN (2012) Double σ–aromaticity in a surface-deposited cluster: Pd$_4$ on TiO$_2$ (110). J Phys Chem Lett 3:751–754

41. Zhang L, Wu P, Sullivan M (2011) Hydrogen adsorption on Rh, Ni, and Pd functionalized single-walled boron nitride nanotubes. J Phys Chem C 115:4289–4296